Transactions of the 15th International Conference on
Structural Mechanics in Reactor Technology (SMiRT-15)
Seoul, Korea, August 15-20, 1999

Study on Seismic Performance of Sea Walls, Part 2: The Physical Properties on the Structural Elements of Sea Walls

Setsuo Iizuka[1], Eiji Ohhara[1], Yoshio Suzuki[2], Ryoichi Babasaki[2] and Takaaki Shimizu[2]

1) Nuclear Power Engineering Corporation, Japan
2) Takenaka Corporation, Japan

ABSTRUCT: The objectives of this research are to gain an understanding of the strength and deformation characteristics of the aggregate of armor units in sea walls, and the sliding characteristics between the caisson and mound. This information has been determined necessary to study the seismic performance of sea walls in cases where nuclear power plants are built on man-made islands at sea, as described in Part One. For the experiments, a scale model was used in a centrifugal force field. The tests investigated the relation between shear modulus and shear strain, the relation between dumping ratio and shear strain, and poisson's ratio in an aggregate of armor units. The friction coefficient between caisson and mound was also determined.

1. PHYSICAL PROPERTIES ON THE AGGREGATE OF ARMOR UNITS

1.1 Cyclic simple shear tests

The objective of these tests was to examine the strength and deformation characteristics of armor units.

1.1.1 Shear testing apparatus

The schematic of this apparatus is shown in Fig. 1. This consists of a loading jack, DC servo motor, load cell, shear box, overburden weight (lead shot), and displacement transducer. For the tests, a shear testing apparatus was placed on the platform of a centrifuge apparatus, then a test specimen was installed in the shear box. Cyclic simple shear test was performed under the centrifugal force.

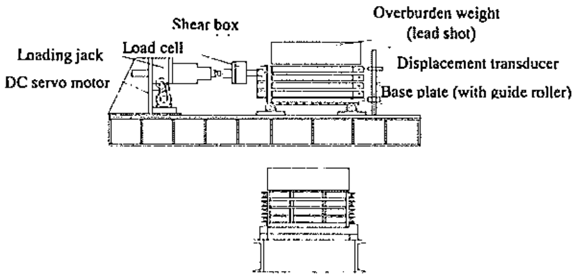

Fig. 1 The schematic of a shear testing apparatus

1.1.2 Test method

An outline of the method is given in Fig. 2. The specimen (50cm long*15cm high*40cm wide) installed in the shear box was subjected to cyclic simple loading at small strain level, and the relation between shear stress and shear strain was determined.

The loading method was stress controlled. Cyclic loading was sine wave of 12 cycles, and the frequency of the load was 0.1Hz. The cyclic stress level was increased at each step.

Shear stress was calculated from measurements of the load. Shear strain was calculated from measurements of horizontal displacement at the top of the loading plate of the shear box. Using the 5th and 10th wave from the time histories of shear stress and shear strain measured at each loading step, the relation between the shear modulus and shear strain, and between the dumping ratio and shear strain, were determined for an aggregate of armor units.

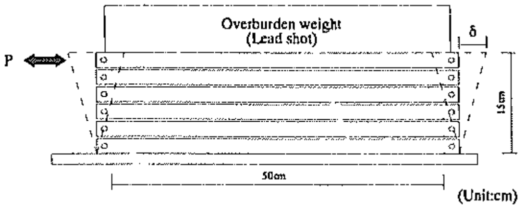

Fig. 2 Outline of cyclic simple shear tests

1.1.2 Test conditions

The test conditions are described in Part1. Confining pressure, unit size, and unit shape were selected as parameters, and their effects on the test results were examined. For the confining pressure, the armor units in the section shown in Fig. 3 were divided into three layers. The test condition was determined to the pressure confined to each layer. As the sizes of armor units using for actual projects, 80, 40 and 16 tons were selected, and for the tests 1/100 scale models of the 80 ton type were used. The effect of different sized units was obtained by varying the centrifugal acceleration applied to the specimen, as shown in Table 1. Two shapes of armor unit were selected: one that is widely used, and another of differing shape characteristics. The test specimen consists of armor units piled at random in dry condition, and porosity of the test specimen was 0.5.

1.1.3 Test results

The relation between shear strain and shear modulus and between shear strain and dumping ratio are shown in Figs. 4 to 6. In each case it was confirmed that both shear modulus and dumping ratio in an aggregate of armor units varied with an increase in strain, and were found to be strain-dependent to the same extent as the soil material. Fig. 4 shows that the higher the confining pressure the larger the shear modulus. However, the dumping ratio showed no dependence on the confining pressure. In both cases, at a strain level in the order of 10^{-5}, the data is dispersed. The cause for this is thought to be that as cyclic simple shear tests cause forced shear deformation by contact pressure on the specimen, the loading plate may easily have some effect and lead to a distorted distribution of strain. Fig. 7 shows a time history and hysteresis loops of stress and strain at a strain level of the order of 10^{-5}. As residual strain can be observed in the specimen, this is thought not to be the behavior of the aggregate, but due to a localized rearrangement of armor units. Above strain levels of $5.0*10^{-3}$ the dumping ratio declines. The cause of this is thought to be that as the strain level increases, the armor units are damaged and compacted. Fig.5 shows that the shear modulus and dumping ratio of the aggregate of armor units is not greatly dependent on unit size. Fig. 6 shows that compared with the Type1, the shear modulus is larger and the dumping ratio is smaller in the Type2. This is thought to be due to differences in the amount of free space created between the units, rather than the shape characteristics of the units. In the Type2 the void within each unit is fixed, so there is less scope for free space than in the Type1; as a result the aggregate shear modulus is large and the dumping ratio is small.

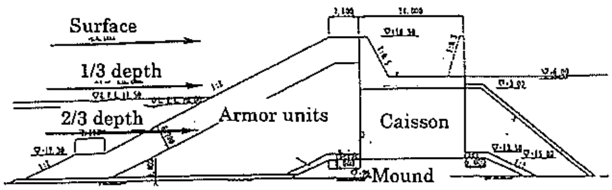

Fig. 3 Study section of sea wall

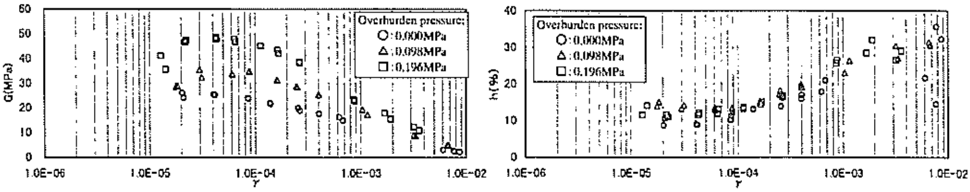

(1) Relation between shear strain γ and shear modulus G

(2) Relation between shear strain γ and dumping ratio h

Fig. 4 Effect of confining pressure (80ton Type1 units)

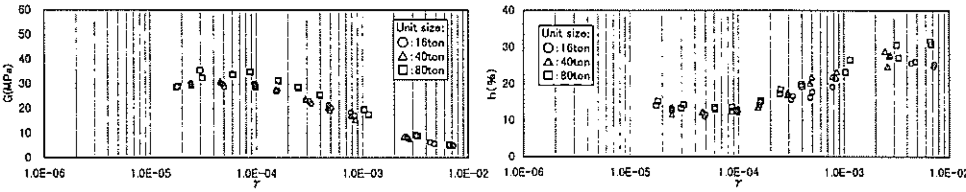

(1) Relation between shear strain γ and shear modulus G

(2) Relation between shear strain γ and dumping ratio h

Fig. 5 Effect of armor unit size (Type1 units, overburden pressure is 0.098MPa)

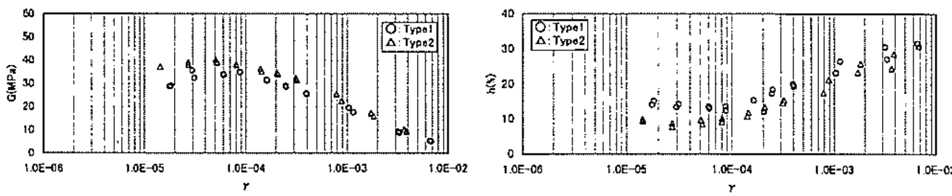

(1) Relation between shear strain γ and shear modulus G

(2) Relation between shear strain γ and dumping ratio h

Fig. 6 Effect of armor unit shape (80ton units, overburden pressure is 0.098MPa)

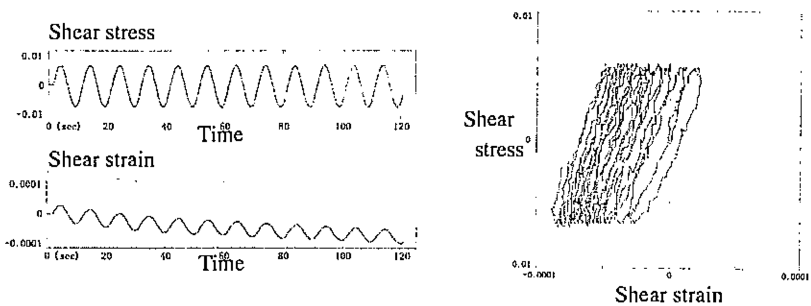

Fig. 7 Shear stress and shear strain at very small strain level

1.2 Shear tests at very small strain level

The objective of these tests was to examine shear modulus at very small strain level in an aggregate of armor units.

1.2.1 Test method

An outline of the test method is shown in Fig. 8. Models of armor units were piled at random in a container to form an embankment shape 45cm in height. The container was set on the shaking table, and micro-amplitude transverse wave input from below. Measurements were taken with accelerometer located at the top and bottom of the specimen. Fig. 9 shows how the test results were processed. The transverse wave velocity was calculated from the difference in arrival times of the first wave, taken from acceleration time histories for each accelerometer. Then the transverse wave velocity was substituted in the equation $G=\rho*Vs^2$, (where G is the shear modulus, ρ is the specimen density, and Vs is the transverse wave velocity) and the shear modulus was calculated. The shear strain was calculated by integrating the measured accelerations and determining the displacement, and dividing the relative horizontal displacement between the measured points by the distance between the points.

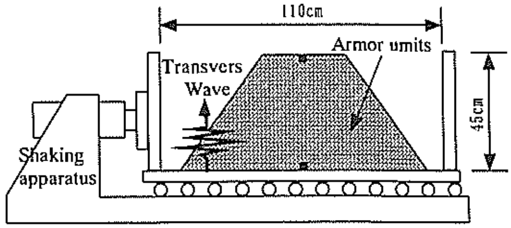

Fig. 8 Outline of shear tests at very small strain level

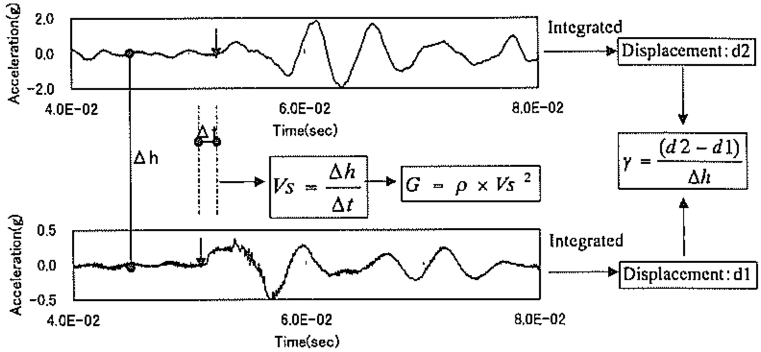

Fig. 9 Processing of test results

1.2.2 Test conditions

The test conditions are shown in Table 1. Only models of Type1 armor units were used.

Table 1 Test conditions

Specimen	Density	1.15 ton/m^3 (porosity is 50%)
	Height	45 cm
Input motion	Input method	transverse wave (1 wave) using a shaking table
	Frequency	200 Hz
	Amplitude	1.0 G
Sampling	Frequency	20 kHz
Centrifugal acceleration		57g, 77g, 100g

1.2.3 Test results

The test results are shown in Table 2 and Fig.10. The transverse wave velocity ranged between 220 to 310m/sec. Shear strain was extremely small, in the order of 10^{-8}. The shear modulus obtained from these tests was 2 to 3 times larger than the initial shear modulus determined through cyclic simple shear tests. As in the results of the cyclic simple shear tests, the shear modulus was not found to be dependent on armor unit size.

Table 2 Transverse wave velocity

Test case	Armor unit Size (ton)	Transverse wave velocity (m/sec)
S57-1	16	265
S57-2		281
S57-3		220
S77-1	40	273
S77-2		257
S77-3		273
S100-1	80	273
S100-2		310
S100-3		237

1.3 Poisson's ratio tests

The objective of these tests was to examine Poisson's ratio for an aggregate of armor units.

1.3.1 Test method

An outline of the test method is shown in Fig. 11. Armor units were piled at random in a container to make an embankment shape 45cm in height. A steel plate was placed on the top of the specimen, which was subjected to micro-amplitude longitudinal waves through the free fall of a rammer. Accelerometers were located at the top and bottom of the specimen and measurements were taken. Fig. 12 shows how the test results were processed. The longitudinal wave velocity was calculated from the difference in arrival times of the first wave, taken from acceleration time histories for each of the measuring points. Then the longitudinal wave, and the transverse wave determined in 1.2, were substituted in the equation $\nu = \{(V_p/Vs)^2-2\}/2\{(V_p/Vs)^2-1\}$ (where ν is Poisson's ratio, V_p is the longitudinal wave velocity, Vs is the transverse wave velocity), and Poisson's ratio ν was calculated.

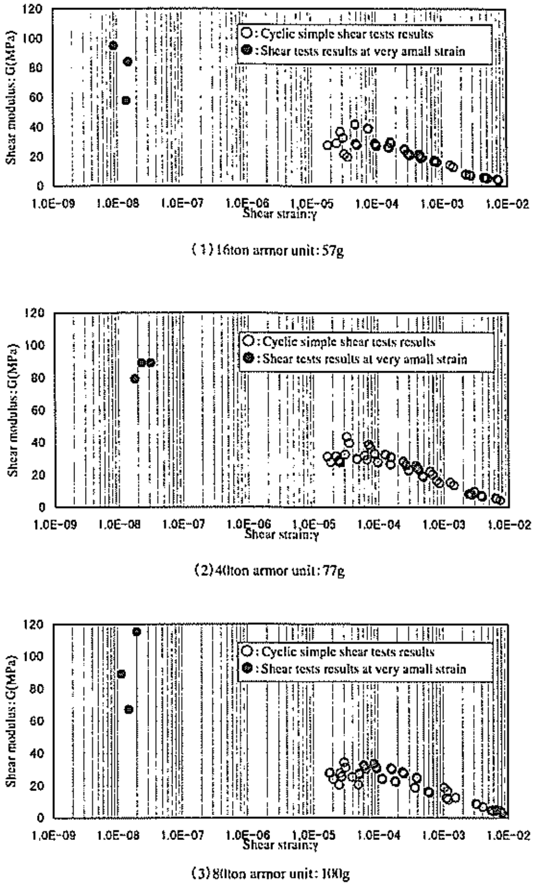

Fig. 10 Relation between shear strain and shear modulus

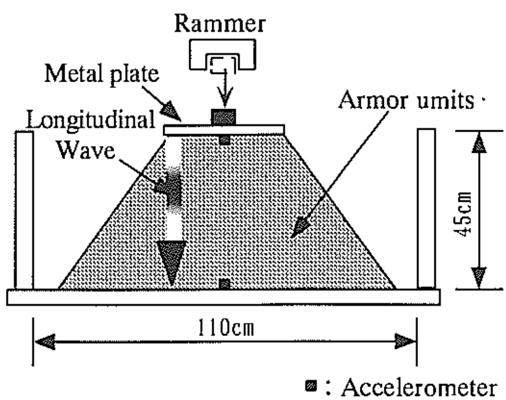

Fig. 11 Outline of poisson's ratio test

1.3.2 Test conditions

The test conditions are shown in Table 3. Specimen and centrifugal acceleration are same as Table 1.

1.3.3 Test results

The test results are shown in Table 4. The longitudinal wave velocity ranged between 600 and 847m/sec. Poisson's ratio was found to be between 0.38 and 0.45 and was not dependent on unit size. At the very small strain level, the aggregate of armor units is linear elasticity, and because their shape enables the armor units to mesh well with each other, realignment is unlikely to occur. However, the armor units are the material with particle breakage, causing damage to the armor units, so as the strain level increases plastic deformation occurs, and Poisson's ratio may be expected to gradually decline.

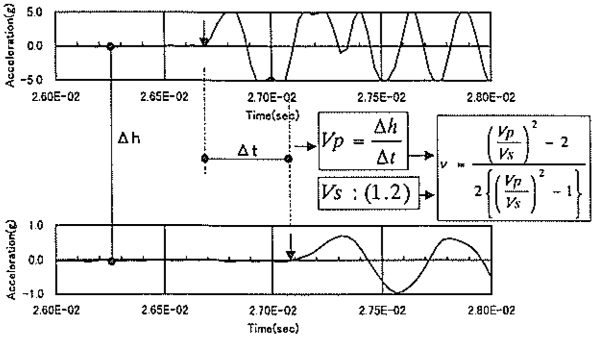

Fig. 12 Processing of test results

Table 3 Test conditions

Input motion	Input method	longitudinal wave using a rammer
	Amplitude	1.0 G
Sampling	Frequency	32 kHz

Table 4 Poisson's ratio

Test case	Unit size (ton)	Longitudinal wave velocity (m/sec)	Poisson's ratio
P57-1		600	0.38
P57-2	16	626	0.37
P57-3		758	0.45
P77-1		626	0.38
P77-2	40	720	0.43
P77-3		655	0.39
P100-1		847	0.44
P100-2	80	847	0.42
P100-3		686	0.43

2. SLIDING TESTS BETWEEN CAISSON AND MOUND

2.1 Friction tests between caisson and mound

The objective of these tests was to examine the skin friction coefficient between the bottom surface of the caisson and the top of the mound.

2.1.1 Test method

An outline of the test method is shown in Fig. 13. In a container, mound model in which mound material was fixed with cement to prevent deformation, and a mound model with consistent surface roughness was created. A caisson model was placed on top of the mound and horizontal loading was applied with a load cell. Load, and horizontal and vertical displacements of the caisson were measured, the relation between the load and the sliding resistance was determined and the friction coefficients calculated.

2.1.2 Test conditions

The test conditions are shown in Table 5. The models of the caisson and mound were 1/100 scale models taken from the study section of sea wall shown in Fig. 3.

2.1.2 Test results

The relation between the horizontal displacement of the caisson and sliding resistance is shown in Fig.14. No peak was observed in the sliding resistance on the first loading, but from the second loading on, peaks were observed. As shown in Fig. 15, the initial sliding resistance was assessed using the peak sliding resistance while the caisson was at rest. No peaks were observed in the sliding resistance while the caisson was sliding, and so 10 points of the almost constant sliding resistance were selected and their average value was assessed.
The results found the static coefficient of friction to be 0.69 and the dynamic coefficient of friction to be 0.64.

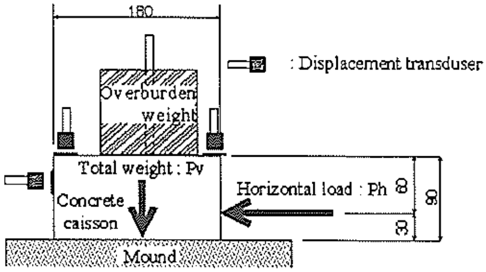

Fig. 13 Outline of friction tests between caisson and mound

Table 5 Test conditions

Centrifugal acceleration		100g
Mound	Model	Fixed with cement
	Material	Diameter 5-18mm Uc=1.95
Caisson model	Material	Concrete (ρ=2.3ton/m^3)
	Contact pressure	200,400,1000kN/m^2
Horizontal Loading	Method	Unidirectional loading
	Velocity	1 mm/min

2.2 Sliding tests between caisson and mound

The objective of these tests was to examine the sliding characteristics of the caisson that included the shear deformation of the mound.

2.2.1 Test method

An outline of the test is shown in Fig. 16. The container, caisson model and measuring equipment were mostly the same as those described in 2.1.1. However, in these tests the mound material was not fixed, and the model allowed for shear deformation of the mound as well as sliding of the caisson. Located on top of the mound, the caisson was subjected to horizontal loading, and the load, and horizontal and vertical displacement of the caisson were measured. As in 2.1, the relation between the load and sliding resistance was determined and the friction coefficients calculated.

2.2.2 Test conditions

The test conditions were as shown in Table 5. The mound was 5cm thick (1/100 the size of the prototype), and was created in three relative densities of 60%,

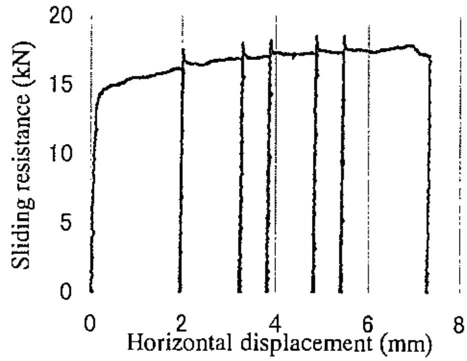

Fig. 14 Relation between horizontal displacement of caisson and sliding resistance

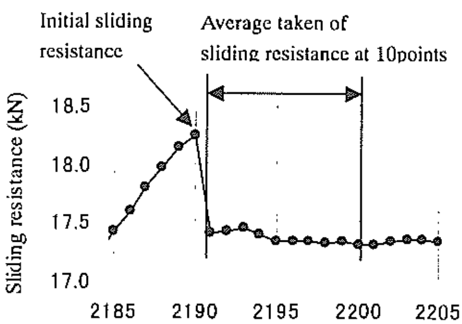

Fig.15 Method of assessing measured results

80% and 110%.

2.2.3 Test results

Fig. 17 shows the relation between the horizontal displacement of the caisson and the sliding resistance. On the first loading, about 10mm of horizontal displacement was needed before maximum sliding resistance was reached, but from the second loading on, the maximum sliding resistance was reached on less than 1mm of displacement. On the first loading, the larger the relative density of the mound, the larger the sliding resistance, but from the 2nd loading on, no difference was observed in the sliding resistance resulting from different relative densities. This is thought to be because the first loading compacted the mound material, so despite their initial difference, from the second loading on the relative densities were the same. Fig. 18 shows the relation between the load and sliding resistance, obtained from the tests in 2.1 and 2.2. The friction coefficient obtained in the sliding tests between caisson and mound was 0.63, which was in the same order as the dynamic coefficient of friction obtained from the friction tests between caisson and mound. Thus it appears that the initial displacement of the caisson is largely due to shear deformation in the mound material, but as the sliding resistance approaches its maximum value, the mound material has become compacted, and the caisson slides dependent on skin friction with the mound.

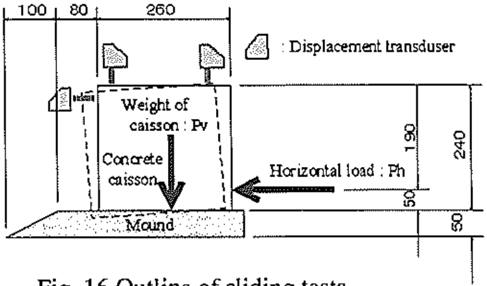

Fig. 16 Outline of sliding tests between caisson and Mound

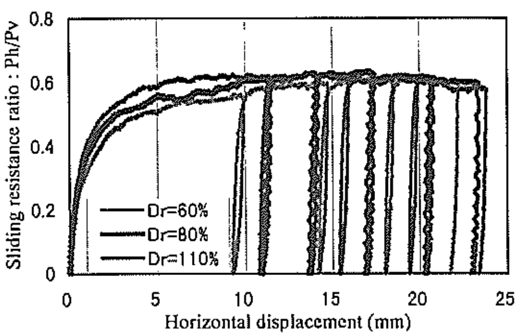

Fig. 17 Relation between horizontal displacement and sliding resistance of caisson

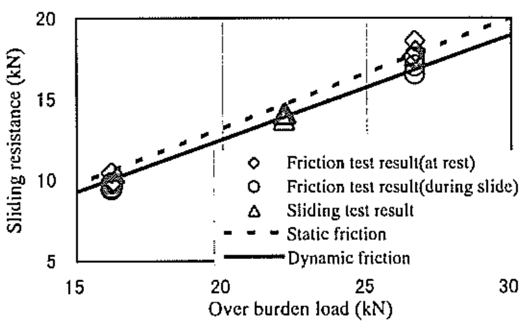

Fig. 18 Relation between overburden load and sliding resistance

3. CONCLUSION

Centrifugal model tests were performed, so the strength and deformation characteristics of armor units and the sliding characteristics between caisson and mound were obtained. They are for the seismic design of sea walls when nuclear power plants are built on man-made islands at sea. But it is necessary to consider the poisson's ratio of armor units at large strain level, and the effect of water.